Part I

Signals, spectra and optical modulations

1 Baseband signals and power spectra

The theorem of conjugated pulses and its application to the raised cosine autocorrelator

1.1 Introduction

In this chapter, we will review some relevant results of the spectral analysis of random signals, in particular the matched filter with the raised cosine output response. Owing to the characteristic property of every matched filter of generating an output pulse which is the same as the autocorrelation of the input pulse, we will present a detailed analysis of the raised cosine autocorrelator. This system represents in fact the optimum receiving filter for the given input additive white noise, providing at the same time the maximum signal-to-noise power ratio and the absence of any intersymbol interference (ISI). The raised cosine autocorrelator showing the minimum noise bandwidth is the well-known Nyquist receiver. It has a frequency response identical to the ideal frequency window of width equal to the reciprocal of the bit time. These concepts represent a valuable background well suited for the modeling and comparison of different transmission systems and photoreceiver architectures. The following sections illustrate some applications of the raised cosine autocorrelator in conjunction with specific optical modulation formats.

Section 1.2 presents the differential encoding technique, which is extensively used in the optical demodulation of differential phase shift keying (DPSK) and differential quadrature phase shift keying (DQPSK) signals. After introducing the operating principle, the section proceeds with the analysis of the encoding and decoding algorithms, showing simple circuit realizations. Section 1.3 reviews basic results concerning the autocorrelation, the power spectrum and the average power of random sequences of arbitrary pulses. Section 1.4 presents the average power theorem of conjugated pulses as a consequence of Parseval's theorem and the symmetry property of the Fourier transform pair. The average power theorem is useful in the calculation of the average power of uncorrelated sequences of conjugated pulses, without providing the explicit solution of the integral forms. The raised cosine pulse and the ideal square pulse, in their respective conjugated domains, are illustrated as simple analytical applications of the average power theorem. The section closes with several simulations of the raised cosine pulse and of the error function pulse.

Sections 1.5 and 1.6 deal with the important concept of uncorrelated random sequences characterized by the raised cosine power spectrum. The generating pulse is shaped like the inverse Fourier transform of the square root of the raised cosine spectrum and it is proportional to the impulse response of the raised cosine autocorrelator. The analytical form of the noise bandwidth of the raised cosine autocorrelator and the calculation of the

signal-to-noise ratio close the section. Finally Section 1.7 provides time- and frequency-domain characterization of the single-pole, Gaussian and Bessel–Thompson responses up to the eighth order, concluding with a comparison among their respective noise bandwidths.

1.2 Differential encoding

Although various signal shapes, generated by different optical modulations, will be analyzed in the following chapters, it is beneficial to introduce differential encoding of the binary data stream in this context, where more general baseband signals and spectra will be approached. Differential encoding is a widely used signal pre-processing which allows direct demodulation of the phase-modulated signals, overcoming the phase ambiguity problem and without considering the more sophisticated coherent demodulation. Differential encoding is indispensable for the direct detection of phase shift keying (PSK) and quadrature phase shift keying (QPSK) modulated fields as it provides a simple encoding procedure that allows symbol recovery at the receiver end, without suffering the phase ambiguity problem and circumventing more sophisticated coherent detection schemes. Today, differential encoding is successfully implemented in all PSK and QPSK optical transmission systems that do not rely on the coherent detection architecture. In other words, we could consider differential encoding and the coherent detection scheme as competing architectures for the realization of an optical fiber transmission system based on phase modulations.

The strength of differential encoding relies on the simplicity of implementation of both encoder and decoder circuits, even if it does not allow any compensation algorithm for overcoming transmission impairments as performed indeed by the more complex DSP (digital signal processing) based coherent optical demodulation schemes. In particular, differential decoding is somehow a remarkable intrinsic property of both PSK and QPSK photoreceivers based on the simple delay-line interferometer (DLI). In order to distinguish between standard PSK modulation and the differentially encoded PSK, it is customary to add the letter "D" in front of the phase modulation acronym. Thus we will indicate by DPSK and DQPSK, respectively, the standard PSK and QPSK optical modulations where the signal data stream has been differentially encoded before being applied to the optical modulator.

1.2.1 The differential encoder

The principle of the differential encoder is described by two rules:

S.1 *Maintain the logic value of the previous bit each time the input bit assumes a logic low.*

S.2 *Make a logical transition with respect to the previous bit each time the input bit assumes a logic high.*

It should be apparent that if the input bit $a_n = 0$, the differentially encoded output bit b_n maintains the same logic level as b_{n-1}; otherwise it assumes the complementary logic state. Conversely, when the input bit goes to the high level, the differential encoded output bit b_n makes a transition to the complementary logic state b_{n-1}:

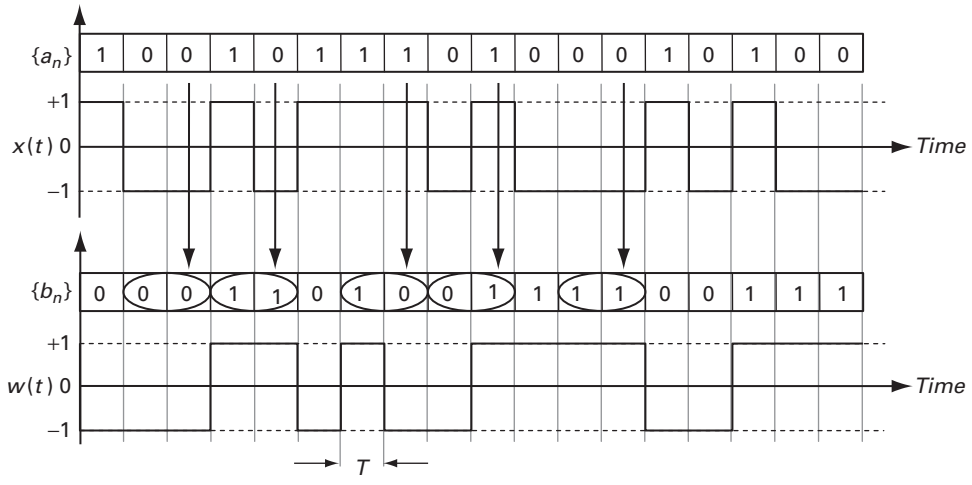

Figure 1.1 Temporal representation of differential encoding operating on the input sequence $\{a_n\}$.

$$\text{Differential encoding:} \quad \begin{cases} a_n = 0 & \Rightarrow \quad b_n = b_{n-1} \\ a_n = 1 & \Rightarrow \quad b_n = \overline{b_{n-1}} \end{cases} \tag{1.1}$$

In other words, the output bit toggles the logic level every time the input bit goes high and it remains on the same level when the input bit goes low. The essential principle of differential encoding applied to binary signals can be summarized as follows:

S.3 *Information content is transferred from the logic level to the presence or absence of transitions between consecutive logic levels.*

Accordingly, when two consecutive symbols b_{n-1}, b_n of the differentially encoded stream $\{b_n\}$ assume the same level, the current input a_n is necessarily in the low state. Conversely, when two consecutive symbols b_{n-1}, b_n toggle the level, the current input a_n is necessarily in the high state. Figure 1.1 shows the differential encoding of the $\{a_n\}$ input sequence, assuming ideal not-return-to-zero (NRZ) square-shaped pulses.

The differential encoding rule is represented by the following truth table:

a_n	b_{n-1}	b_n
0	0	0
0	1	1
1	0	1
1	1	0

(1.2)

The truth table (1.2) is realized with the modulo-2 adder (EXOR logic) according to the following *differential encoding* equation and the schematic circuit reported in Figure 1.2:

$$b_n = a_n \oplus b_{n-1} \tag{1.3}$$

1.2.2 The differential decoder

The differential decoder performs the inverse operation of the differential encoder, restoring at the output the original sequence $\{a_n\}$. To this end, we report in

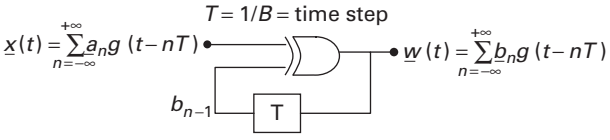

Figure 1.2 Circuit diagram of the ideal modulo-2 adder for the implementation of the differential encoder.

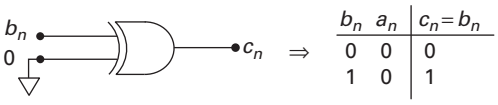

b_n	a_n	$c_n = b_n$
0	0	0
1	0	1

Figure 1.3 Identity element of the modulo-2 adder realized with EXOR.

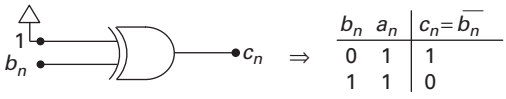

b_n	a_n	$c_n = \overline{b_n}$
0	1	1
1	1	0

Figure 1.4 Complementary element of the modulo-2 adder realized with EXOR.

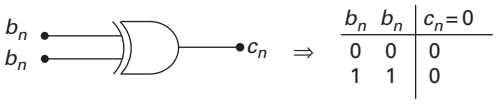

b_n	b_n	$c_n = 0$
0	0	0
1	1	0

Figure 1.5 Low-logic element of the modulo-2 adder realized with EXOR.

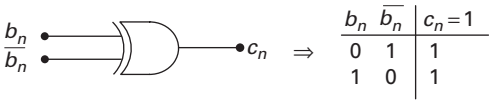

b_n	$\overline{b_n}$	$c_n = 1$
0	1	1
1	0	1

Figure 1.6 High-logic element of the modulo-2 adder realized with EXOR.

Figures 1.3 to 1.6 four properties of the modulo-2 adder together with their respective circuit realizations:

$$\text{Identity element:} \quad b_n \oplus 0 = b_n \tag{1.4}$$

$$\text{Complementary element:} \quad b_n \oplus 1 = \overline{b_n} \tag{1.5}$$

$$\text{Low-logic element:} \quad b_n \oplus b_n = 0 \tag{1.6}$$

$$\text{High-logic element:} \quad b_n \oplus \overline{b_n} = 1 \tag{1.7}$$

In addition to the above identities, note also the associative property:

$$(a_n \oplus b_n) \oplus c_n = a_n \oplus (b_n \oplus c_n) \tag{1.8}$$

The associative property can be easily verified with the aid of the truth table in (1.2):

a_n	b_n	c_n	$(a_n \oplus b_n) \oplus c_n$	$a_n \oplus (b_n \oplus c_n)$
0	0	0	0	0
0	0	1	1	1
0	1	0	1	1
0	1	1	0	0
1	0	0	1	1
1	0	1	0	0
1	1	0	0	0
1	1	1	1	1

(1.9)

In order to retrieve the original sequence $\underline{a}_n$, it is sufficient to perform the modulo-2 addition between sequences $\underline{b}_n$ and $\underline{b}_{n-1}$. In fact, after substituting for $\underline{b}_n$ the differential encoding equation (1.3), and applying consecutively the associative property (1.8) and the identities (1.6) and (1.4), we obtain the original sequence:

$$b_n \oplus b_{n-1} = \Big|_{b_n = a_n \oplus b_{n-1}} \quad (a_n \oplus b_{n-1}) \oplus b_{n-1} = a_n \oplus (b_{n-1} \oplus b_{n-1}) = a_n \oplus 0 = a_n \tag{1.10}$$

Figure 1.7 shows a schematic diagram of the differential decoder, according to the procedure shown in (1.10). The same figure shows in the upper part the complete differential codec block diagram, including only one delay time. However, the differential encoder and decoder operations are usually performed upon bidirectional data fluxes and they cannot be simply cascaded. Accordingly, Figure 1.7 shows in the lower part the individual encoder and decoder schematics.

In order to have consistent timing between the input sequence and the single-time-step delayed sequence, it is advisable to use a clocked delay line in the differential

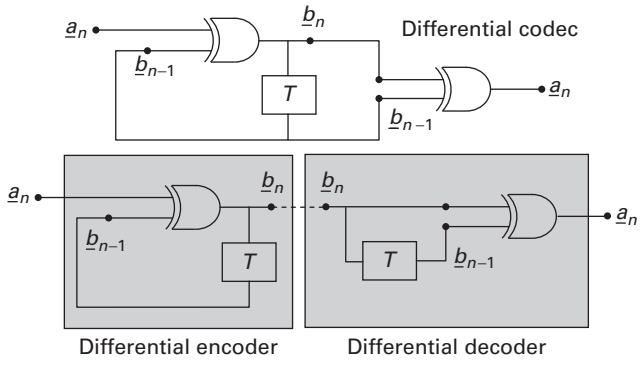

Figure 1.7 Circuit diagram of the differential decoder. At the top is the cascaded codec configuration, using only one delay line shared between the encoder and the decoder session. At the bottom are the individual block diagrams of the differential encoder and decoder sessions.

encoder and decoder. To this end, the delay line T must be replaced with a D-type flip-flop (D-FF), with the same clock used for generating the data sequence. We note that the D-FF operates synchronously with the clock edges. Usually, the input data are gathered during the rising edge of the clock pulse, and they are released synchronously with the output during the subsequent falling edge. In order to acquire correctly the input data, the latter must be stable during the preset and hold time intervals across the rising edge of the clock pulse. Accordingly, the design of both circuits must include the accurate analysis of the signal propagation times, both in the clocked D-FF as well as in the asynchronous EXOR port. In clocked implementation, data sequences at both input ports of the EXOR will be available with the appropriate timing, avoiding false transitions and related code errors.

1.3 Random sequences and power spectra

In this section, we will discuss some relevant results of the spectral analysis [1]. With the sequence $\{a_n\}$ of real numbers, we form the clocked impulse sequence $s(t)$, with time step T:

$$s(t) = \sum_{n=-\infty}^{+\infty} a_n \delta(t - nT) \tag{1.11}$$

The autocorrelation $R_s(t)$ of the impulse sequence (1.11) is also a sequence of impulses with real coefficients A_n:

$$R_s(t) \triangleq \lim_{\sigma\to\infty} \frac{1}{2\sigma} \int_{-\sigma}^{+\sigma} s(t+\tau)s^*(\tau)d\tau \quad \Rightarrow \quad R_s(t) = \frac{1}{T} \sum_{n=-\infty}^{+\infty} A_n \delta(t - nT) \tag{1.12}$$

where

$$A_n = \lim_{k\to\infty} \frac{1}{2k} \sum_{m=-k}^{+k} a_m a_{m+n} \tag{1.13}$$

The left side of (1.12) is the definition of the autocorrelation of finite power signals. As can be easily demonstrated, the coefficients A_n in (1.13) satisfy the symmetry condition

$$A_{-n} = A_n \tag{1.14}$$

From (1.12) and (1.14), we conclude that the power spectrum $S_s(f)$ of the impulse sequences $S(t)$ in (1.11) is the following real and even periodic function of the frequency:

$$S_s(f) = \frac{A_0}{T} + \frac{1}{T} \sum_{n=1}^{+\infty} A_n \left(e^{+jn2\pi fT} + e^{-jn2\pi fT}\right) = \frac{A_0}{T} + \frac{2}{T} \sum_{n=1}^{+\infty} A_n \cos n2\pi fT \tag{1.15}$$

Let us consider below some relevant applications.

1.3.1 Uncorrelated random sequence of impulses

We assume that the random sequence $\{\underline{a}_n\}$ of real coefficients is uncorrelated in the sense that it satisfies the following conditions:

$$\{\underline{a}_n\}: \begin{cases} \lim_{k\to\infty} \frac{1}{2k} \sum_{m=-k}^{+k} \langle a_m a_{m+n} \rangle = 0 & , \quad \forall n \neq 0 \\ \lim_{k\to\infty} \frac{1}{2k} \sum_{m=-k}^{+k} \langle a_m^2 \rangle = A^2 & , \quad a_m = [-A, +A] \end{cases} \tag{1.16}$$

with A a real positive constant:

$$\underline{s}(t) = \sum_{n=-\infty}^{+\infty} \underline{a}_n \delta(t - nT) \tag{1.17}$$

The first requirement in (1.16) represents the uncorrelation condition, while the second one specifies the energy of the single impulse of the sequence (1.11). For the uncorrelated sequence $\{\underline{a}_n\}$ satisfying (1.16), the coefficients A_n in (1.13) must be identically null, except for $n = 0$, where $A_0 = A^2$. Consequently, the autocorrelation (1.12) of the random sequence (1.17) of uncorrelated impulses coincides with the single impulse at the time origin:

$$R_{\underline{s}}(t) = \frac{A^2}{T} \delta(t) \tag{1.18}$$

From (1.18), we conclude that the power spectrum $S_{\underline{s}}(f)$ of the uncorrelated impulse sequences $\underline{s}(t)$, whose coefficients satisfy (1.16), assumes a constant value (white spectrum):

$$S_{\underline{s}}(f) = \frac{A^2}{T} \tag{1.19}$$

1.3.2 Uniform sequence of impulses (comb spectrum)

The second example we will consider deals with a uniform sequence of equidistant impulses. In a sense this is the complementary case to the random sequence we analyzed in Section 1.3.1. From (1.19) we concluded that the power spectrum of random uncorrelated impulses is constant over the whole frequency axis, leading to the concept of a "white noise" process. In the current case of a uniform sequence of impulses, we assume that the sequence $\{\underline{a}_n\}$ consists of constant coefficients for every index n. Setting $a_n = A$, $s(t)$ in (1.11) reduces to the deterministic uniform sequence of impulses with constant area (comb signal):

$$s(t) = A \sum_{n=-\infty}^{+\infty} \delta(t - nT) \tag{1.20}$$

From (1.13), we deduce easily that all coefficients A_n of the autocorrelation function $\rho_s(t)$ are equal to the constant A^2:

$$A_n = A^2 \lim_{k\to\infty} \frac{1}{2k} \sum_{m=-k}^{+k} m = A^2 \tag{1.21}$$

Substituting (1.21) into (1.12), we conclude that the autocorrelation function is the sequence of equidistant impulses with constant area A^2/T:

$$R_s(t) = \frac{A^2}{T} \sum_{n=-\infty}^{+\infty} \delta(t - nT) \tag{1.22}$$

Furthermore, the power spectrum of the uniform sequence of impulses is given by the Fourier transform of (1.22):

$$S_s(f) = \frac{A^2}{T} \sum_{n=-\infty}^{+\infty} e^{jn2\pi fT} \tag{1.23}$$

Finally, using the well-known result [1]

$$\sum_{n=-\infty}^{+\infty} e^{jn2\pi fT} = \frac{1}{T} \sum_{n=-\infty}^{+\infty} \delta(f - n/T) \tag{1.24}$$

we conclude from (1.23) that the power spectrum of $S(t)$ is a uniform sequence of equidistant frequency impulses, spaced by $1/T$ (see Figure 1.8):

$$S_s(f) = \frac{A^2}{T^2} \sum_{n=-\infty}^{+\infty} \delta(f - n/T) \tag{1.25}$$

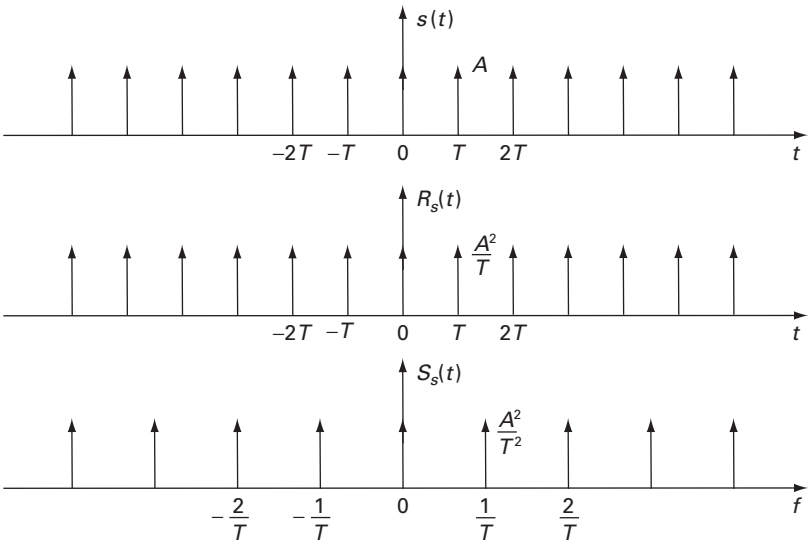

Figure 1.8 The autocorrelation $\rho_s(t)$ of the sequence $s(t)$ of equidistant impulses of constant area A is also a sequence of impulses with the same time step T and area A^2/T. The power spectrum is also a sequence of equidistant impulses of frequency step $1/T$ and area A^2/T^2.